10.1109/ULTSYM.2012.0531

Improved Visualization of Endocardial Borders with Short-Lag Spatial Coherence Imaging of Fundamental and Harmonic Ultrasound Data

Muyinatu A. Lediju Bell[1], Robi Goswami[2], Jeremy J. Dahl[1], and Gregg E. Trahey[1,3]
[1]Department of Biomedical Engineering, Duke University, Durham, NC, USA
[2]Department of Cardiology, Duke University, Durham, NC, USA
[3]Department of Radiology, Duke University Medical Center, Durham, NC, USA

Abstract— **Endocardial border visualization, a common task in echochardiography, is typically challenged by the presence of acoustic clutter. This study investigates endocardial border visibility in co-registered fundamental and harmonic data when utilizing the Short-Lag Spatial Coherence (SLSC) beamformer, a clutter reduction approach that we developed. Individual channel echo data were acquired from the left ventricle of 12 volunteers, after informed consent and IRB approval, to create matched image quadruplets of fundamental and harmonic B-mode and SLSC images. Contrast-to-noise ratios (CNR) were measured, and three cardiologists rated the visibility of endocardial segments in randomly ordered cine loops. The statistical significance of visibility ratings was determined with a Holm-Bonferroni correction at a significance level, $\alpha = 0.05$. CNR increased approximately two-fold in fundamental and harmonic SLSC images compared to fundamental and harmonic B-mode images. Fundamental and Harmonic SLSC imaging offered the greatest benefits when fundamental B-mode image quality was poor. Improvements in endocardial segment visibility in short-axis views ranged from 16-28% ($\alpha = 0.05$) compared to fundamental B-mode images, while improvements in the apical four chamber views ranged from 22-35% ($\alpha = 0.05$) compared to fundamental and harmonic B-mode images. Results suggest that SLSC and HSCI have the potential to increase endocardial border visualization and thereby improve cardiac assessments of poor-quality B-mode images.**

I. Introduction

Echocardiography is routinely used to visualize cardiac anatomy, diagnose heart disease, and characterize abnormalities in cardiac structures. In addition to quantitative measures of cardiac health (i.e. mass, volume, ejection fraction), qualitative assessments of diastolic and systolic wall motion provide useful diagnostic information. Visualization of the left ventricular endocardial border is essential to quantitative and qualitative cardiac analyses [1].

Transthoracic echocardiography with fundamental B-mode imaging offers inadequate visualization of the left ventricular endocardial border in approximately 45-51% of patients [2, 3]. A major source of the inadequate visualization is acoustic clutter. Sources of clutter include reverberations and reflections from extracardiac off-axis structures, such as the ribcage and lungs, as well as from intracardiac structures, such as the chordae tendineae, valves, and myocardial walls [4, 5].

Harmonic imaging is a common approach to improve endocardial border visualization. This technique utilizes the higher harmonics generated by non-linear wave propagation through tissue to create images. Factors that contribute to improved visualization with harmonic imaging include underdeveloped non-linear waves near the transducer surface, minimal harmonic content in reverberant echoes, low amplitude harmonic signals from multiple scattering, suppressed side and grating lobes, and reduced acoustic clutter [6–8]. Harmonic imaging lowered the percentage of patients with inadequate images from 45-51% to 11-24% [2, 3], indicating that harmonic imaging improves image quality in many patients, yet a subset of patients maintain inadequate results with harmonic imaging.

To target the subset of patients that produce inadequate harmonic images, alternative approaches include clutter reduction filters [9–11], transesophageal echocardiography (TEE) [8], and contrast echocardiography [12]. Clutter filters are effective at reducing clutter from stationary or slowly-moving structures, but they have limited ability to remove clutter from higher-velocity sources. TEE requires the oral insertion of an ultrasound probe and provides images with reduced clutter. It poses a discomfort to patients and is only recommended in cases where transthoracic images are diagnostically inconclusive or difficult to acquire [13]. In contrast echocardiography, contrast agents are injected into the patient to distinguish blood from endocardium. Although it is 80-90% effective [14], this approach presents an additional expense to patients and necessitates a sterile environment for intravenous access.

We recently introduced a novel beamforming technique, called Short-Lag Spatial Coherence (SLSC) imaging, that directly forms images based on the local spatial coherence of received ultrasound echoes [15, 16]. This technique is effective because the spatial coherence of echoes returning from the endocardium exhibits different characteristics from clutter and blood echoes [17]. These echo differences are seen in both fundamental and harmonic signals. Similar to the clutter reduction benefits that are associated with harmonic B-mode images, harmonic SLSC images, also referred to as HSCI, have reduced clutter compared to SLSC images created with fundamental data [18]. This study evaluates endocardial visualization in fundamental and harmonic B-mode and SLSC images created from the same echo data.

II. Data Acquisition & Image Processing

A Verasonics™ ultrasound scanner (Redmond, WA) and a 128-element Siemens PH4-1 transducer were utilized to acquire *in vivo* cardiac ultrasound data from 12 volunteers, after IRB approval and informed consent. Short axis and apical four-chamber views of the left ventricle were studied in each volunteer. The volunteers consisted of 6 Duke University employees and 6 patients scheduled for an echocardiogram at the Duke University Medical Center. Clinical echocardiograms were evaluated prior to patient enrollment, and those with good or poor quality images were asked to participate in this study.

The channel data required to make 35 frames of image data were acquired at a rate of approximately 10 frames per second, with an axial sampling frequency of 30 MHz and a transmit frequency of 2 MHz. A pulse-inversion [19] sequence was transmitted to form matched fundamental and harmonic images. Fundamental channel data were formed with echoes received from the normal pulse, and harmonic channel data were formed with summed echoes from the normal and inverted pulses. These ultrasound data were processed offline to create matched fundamental and harmonic B-mode and SLSC images.

One pixel in a fundamental or harmonic SLSC image was formed by computing the short-lag spatial coherence at one depth, n, of the channel signals received by individual transducer elements, using a correlation kernel size ($n_2 - n_1$) of one wavelength. Calculations of spatial coherence are described with the following equations:

$$\hat{R}(m) = \frac{1}{N-m} \sum_{i=1}^{N-m} \frac{\sum_{n=n_1}^{n_2} s_i(n) s_{i+m}(n)}{\sqrt{\sum_{n=n_1}^{n_2} s_i^2(n) \sum_{n=n_1}^{n_2} s_{i+m}^2(n)}}, \tag{1}$$

$$R_{sl} = \sum_{m=1}^{M} \hat{R}(m), \tag{2}$$

where $\hat{R}(m)$ is the normalized spatial coherence measured across a receive aperture [20], N is the number of receive elements, $s_i(n)$ is the time-delayed signal received by the ith element at depth, or time, n, expressed in number of samples, and R_{sl} is the short-lag spatial coherence. SLSC images were created with $M = 15$.

Equations 1 and 2 were implemented at all possible axial and lateral locations to create an SLSC image. Matched B-mode images were constructed by applying a conventional delay-and-sum beamformer to the same channel signals used to make SLSC images. Fundamental images were created by applying the SLSC or delay-and-sum beamformer to fundamental echo signals, while harmonic images were created by applying the beamformers to harmonic signals.

All image processing and data analyses were performed with MATLAB (The Mathworks Inc., Natick, MA) software. Utilizing MEX files and a 3.5-GHz processor, the time to calculate one SLSC image was approximately 2s.

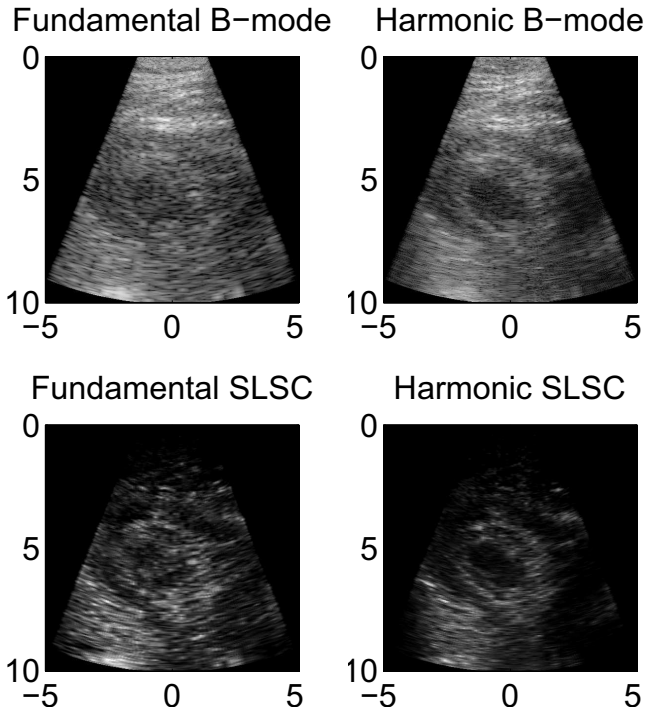

Fig. 1. Short axis views of the left ventricle of Volunteer 10.

TABLE I
MEAN CNR OF THE LEFT VENTRICLE IN THE 12 VOLUNTEERS

	CNR
Fundamental B-mode	0.8
Fundamental SLSC	1.2
Harmonic B-mode	0.8
Harmonic SLSC	1.5

III. Performance Metrics

Contrast-to-noise ratios (CNR) were measured in one image from the short-axis view of each volunteer, using the following equation:

$$\text{CNR} = \frac{|S_v - S_e|}{\sqrt{{\sigma_v}^2 + {\sigma_e}^2}}. \tag{3}$$

where S_v and S_e are the mean signals in the ventricle and endocardium, respectively, and σ_v and σ_e are the standard deviations of signals in the ventricle and endocardium, respectively.

Matched fundamental and harmonic B-mode and SLSC images of the short axis view of the left ventricle of one volunteer are shown in Fig. 1. The fundamental and harmonic SLSC images contain less clutter than the B-mode images, and the left ventricular border is most clearly-defined in the harmonic SLSC image. The mean CNR is approximately a factor of 2 greater in the SLSC images compared to the fundamental and harmonic B-mode images. Mean CNR values for the 12 volunteers are reported in Table I.

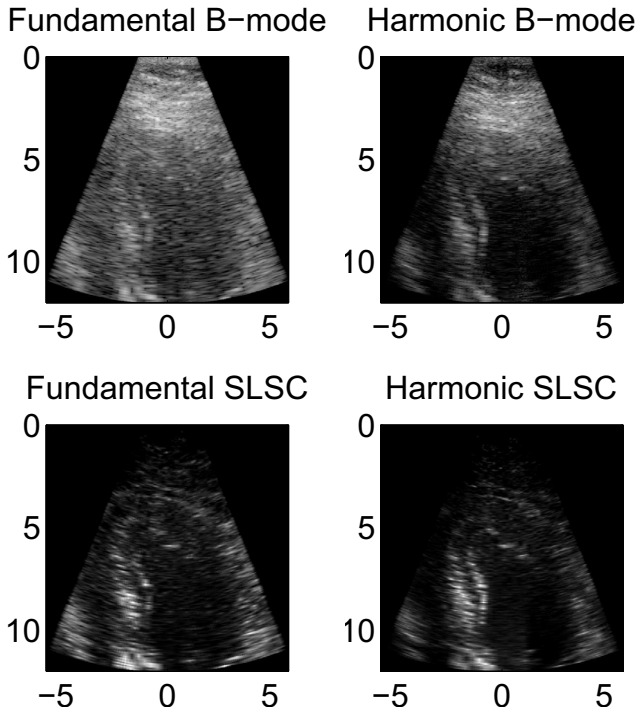

Fig. 2. Apical four-chamber views of the left ventricle of Volunteer 10.

IV. Independent Observer Reviews

Cine loops of the short axis and apical four chamber views were randomized and reviewed independently by three cardiology fellows. The observers were given a segment model that complied with the American Society of Echocardiography standards for short axis and apical four chamber views [21]. There are six segments in the short axis view and seven segments in the apical four-chamber view. Qualitative assessment of endocardial segment visibility during systole and diastole was performed with a visual scoring system ranging from 1 to 3 as follows: 1 = endocardial border clearly visible; 2 = endocardial border visible, but not clearly; and 3 = no endocardial border visible.

The score results from the three cardiologists were separated according to fundamental B-mode image quality, where good was defined as 80% or more of the endocardial segments were visualized by at least two of the three reviewers in systole and diastole (4 volunteers). Poor was defined as less than 80% of the endocardial segments were visualized by at least two of the three reviewers in systole or diastole (8 volunteers). The number of segments not visible in B-mode and SLSC images (score=3) for each image-quality category was compared by a Friedman test to determine if differences existed within each group. Reviewer scores were averaged and statistically significant differences between the means were determined by a paired t-test with a Holm-Bonferroni adjustment to determine statistical significance at a significance level of $\alpha = 0.05$. Improvements were measured as a decrease in the percentage of segments not visualized (score=3), which is the same as an increase in the percentage of visible segments (score=1 or 2).

TABLE II
Statistically significant improvements observed in volunteers with poor-quality fundamental B-mode images

Improvement with	Compared to	Decrease in % of segments not visualized	Ventricular State
Short Axis Views			
HSCI	B-mode	24%	systole
HSCI	B-mode	28%	diastole
SLSC	B-mode	16%	systole
SLSC	B-mode	19%	diastole
Apical 4-Chamber Views			
HSCI	B-mode	33%	systole
HSCI	B-mode	30%	diastole
HSCI	Harmonic	22%	systole
HSCI	Harmonic	23%	diastole
SLSC	B-mode	35%	systole
SLSC	B-mode	31%	diastole
SLSC	Harmonic	24%	systole
SLSC	Harmonic	23%	diastole

The poor-quality B-mode image category contained the most statistically significant differences in segment visibility. Improvements ranged from 16-28% with SLSC and HSCI of the short-axis views, as reported in Table II.

Matched fundamental and harmonic B-mode and SLSC images of the apical four-chamber view of the left ventricle of one volunteer are shown in Fig. 2. The fundamental B-mode image contains the most clutter, and the harmonic B-mode image reduces most of the clutter, except in the proximal region. The fundamental SLSC image reduces much of the near-field clutter, but the apical endocardial borders are not clearly delineated. The harmonic SLSC image contains the least clutter and the most clearly-defined endocardial borders. Statistically significant improvements in segment visibility of the apical four-chamber views ranged from 22-35% with SLSC and HSCI, as reported in Table II. Reviewer scores are summarized in Figure 3.

V. Discussion and Conclusions

CNR was improved and clutter was reduced in a majority of cardiac SLSC images investigated in this study. Results demonstrate that fundamental and harmonic SLSC images offer enhanced visualization of the left ventricular endocardial border. Thus, the implementation of fundamental or harmonic SLSC imaging could likely improve clinical echocardiography assessments of poor-quality B-mode images and increase the detection of cardiac structures or abnormalities that are typically obscured by clutter.

Acknowledgments

This work was supported by the UNCF-Merck Graduate Science Research Dissertation Fellowship and NIH grants R37-HL096023 and R01-EB013661.

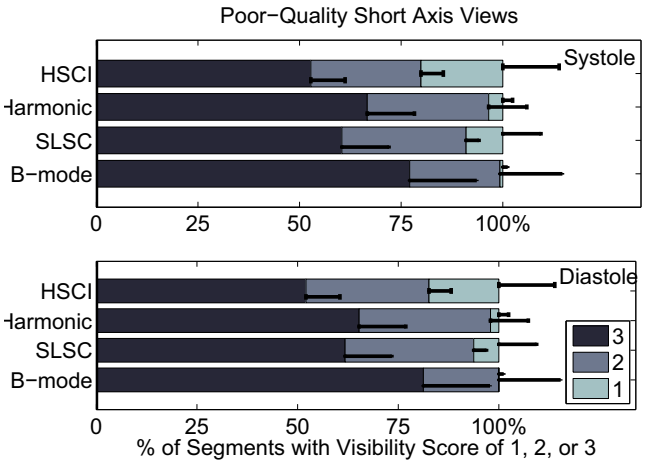

(a)

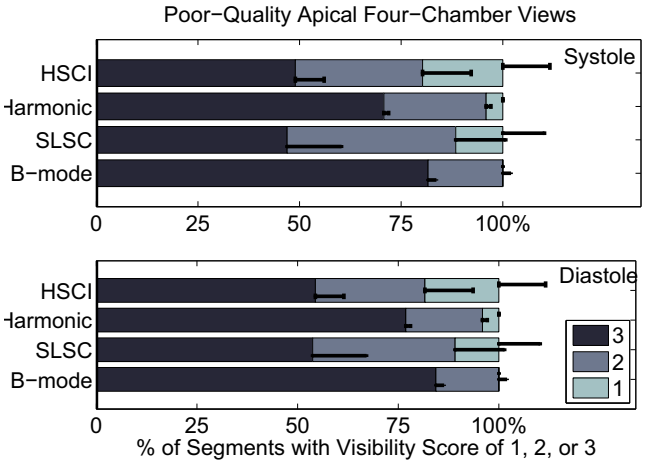

(b)

Fig. 3. Visibility of the LV endocardial segments in poor quality images of the (a) short axis and (b) apical 4-chamber views of the LV. The number of segments with each visibility score (1=clearly seen, 2=poorly seen, 3=not visible) is expressed as a percentage of the total number of segments. The width of the bars represent the mean of the three reviewer scores in systole and diastole and the error bars show one standard deviation. Statistically significant improvements are noted in Table II.

REFERENCES

[1] J. Gottdiener, J. Bednarz, R. Devereux, J. Gardin, A. Klein, W. Manning *et al.*, "American Society of Echocardiography recommendations for use of echocardiography in clinical trials." *Journal of the American Society of Echocardiography*, vol. 17, no. 10, p. 1086, 2004.

[2] F. Chirillo, A. Pedrocco, A. De Leo, A. Bruni, O. Totis, P. Meneghetti, and P. Stritoni, "Impact of harmonic imaging on transthoracic echocardiographic identification of infective endocarditis and its complications," *British Medical Journal*, vol. 91, no. 3, pp. 329–333, 2005.

[3] C. Caiati, N. Zedda, C. Montaldo, R. Montisci, and S. Iliceto, "Contrast-enhanced transthoracic second harmonic echo doppler with adenosine A noninvasive, rapid and effective method for coronary flow reserve assessment," *Journal of the American College of Cardiology*, vol. 34, no. 1, pp. 122–130, 1999.

[4] E. Yeh, "Reverberations in echocardiograms," *Journal of Clinical Ultrasound*, vol. 5, no. 2, 1977.

[5] G. Cloutier, D. Chen, and L. Durand, "A new clutter rejection algorithm for Doppler ultrasound," *IEEE Transactions on Medical Imaging*, vol. 22, no. 4, pp. 530–538, 2003.

[6] F. Tranquart, N. Grenier, V. Eder, and L. Pourcelot, "Clinical use of ultrasound tissue harmonic imaging." *Ultrasound in Medicine and Biology*, vol. 25, no. 6, pp. 889–94, 1999.

[7] F. A. Duck, "Nonlinear acoustics in diagnostic ultrasound." *Ultrasound in Medicine and Biology*, vol. 28, no. 1, 2002.

[8] R. Ward, K. Collins, B. Balasia, K. Spencer, J. DeCara, V. Mor-Avi *et al.*, "Harmonic imaging for endocardial visualization and myocardial contrast echocardiography during transesophageal echocardiography," *Journal of the American Society of Echocardiography*, vol. 17, no. 1, pp. 10–14, 2004.

[9] G. Zwirn and S. Akselrod, "Stationary clutter rejection in echocardiography," *Ultrasound in Medicine and Biology*, vol. 32, no. 1, pp. 43–52, 2006.

[10] F. Mauldin, D. Lin, and J. Hossack, "The Singular Value Filter: A General Filter Design Strategy for PCA-Based Signal Separation in Medical Ultrasound Imaging," *IEEE Transactions on Medical Imaging*, no. 99, pp. 1–1, 2011.

[11] M. A. Lediju, B. C. Byram, and G. E. Trahey, "Sources and characterization of clutter in cardiac B-mode images," in *Proceedings of the IEEE Ultrasonics Symposium*, 2009.

[12] G. Zwirn, R. Beeri, D. Gilon, Z. Friedman, and S. Akselrod, "Quantitative evaluation of local myocardial blood volume in contrast echocardiography," *Medical Image Analysis*, vol. 13, no. 1, pp. 62–79, 2009.

[13] P. Hanrath, "Transoesophageal echo-doppler in cardiology," *British Medical Journal*, vol. 86, no. 5, pp. 586–592, 2001.

[14] L. Crouse, J. Cheirif, D. Hanly, J. Kisslo, A. Labovitz, J. Raichlen *et al.*, "Opacification and border delineation improvement in patients with suboptimal endocardial border definition in routine echocardiography: results of the Phase III Albunex Multicenter Trial," *Journal of the American College of Cardiology*, vol. 22, no. 5, 1993.

[15] M. A. Lediju, G. E. Trahey, B. C. Byram, and J. J. Dahl, "Short-Lag Spatial Coherence of Backscattered Echoes: Imaging Characteristics," *IEEE Transactions on Ultrasonics, Ferroelectrics and Frequency Control*, vol. 58, no. 7, p. 1337, 2011.

[16] M. A. Lediju Bell, R. Goswami, and G. Trahey, "Clutter reduction in echocardiography with short-lag spatial coherence (SLSC) imaging," in *Proceedings of the IEEE International Symposium on Biomedical Imaging*, 2012, pp. 1116–1119.

[17] J. Bamber, R. Mucci, and D. Orofino, "Spatial Coherence and Beamformer Gain," *Acoustical Imaging*, vol. 24, 2000.

[18] J. Dahl, M. Jakovljevic, G. Pinton, and G. Trahey, "Harmonic spatial coherence imaging: An ultrasonic imaging method based on backscatter coherence," *IEEE Transactions on Ultrasonics, Ferroelectrics and Frequency Control*, vol. 59, no. 4, 2012.

[19] A. Vançon, E. Fox, C. Chow, J. Hill, A. Weyman, M. Picard, and M. Scherrer-Crosbie, "Pulse inversion harmonic imaging improves endocardial border visualization in two-dimensional images: comparison with harmonic imaging," *Journal of the American Society of Echocardiography*, vol. 15, no. 4, 2002.

[20] R. J. Fedewa, K. D. Wallace, M. R. Holland, J. R. Jago, G. C. Ng, M. R. Rielly *et al.*, "Spatial coherence of the nonlinearly generated second harmonic portion of backscatter for a clinical imaging system," *IEEE Transactions on Ultrasonics, Ferroelectrics and Frequency Control*, vol. 50, no. 8, 2003.

[21] R. Lang, M. Bierig, R. Devereux, F. Flachskampf, E. Foster, P. Pellikka *et al.*, "Recommendations for chamber quantification: a report from the american society of echocardiography's guidelines and standards committee and the chamber quantification writing group, developed in conjunction with the european association of echocardiography, a branch of the european society of cardiology." *Journal of the American Society of Echocardiography*, vol. 18, no. 12, p. 1440, 2005.